

Strategic advances in formation of cell-in-shell structures: From syntheses to applications



National Research
Foundation of Korea



This paper must be cited as:

Kim, B. J., Cho, H., Park, J. H., Mano, J. F., & Choi, I. S. Strategic advances in formation of cell-in-shell structures: From syntheses to applications. 30(14), 1706063. *Advanced Materials* (2018). <https://doi.org/https://doi.org/10.1002/adma.201706063>

Strategic Advances in Formation of Cell-in-Shell Structures: from Syntheses to Applications

*Beom Jin Kim, Hyeoncheol Cho, Ji Hun Park, João F. Mano, and Insung S. Choi**

((Optional Dedication))

B. J. Kim, H. Cho, Dr. J. H. Park, Prof. I. S. Choi
Center for Cell-Encapsulation Research, Department of Chemistry, KAIST, Daejeon 34141, Korea

E-mail: ischoi@kaist.ac.kr

Prof. J. F. Mano

Department of Chemistry, CICECO - Aveiro Institute of Materials, University of Aveiro, 3810-193 Aveiro, Portugal

Keywords: artificial spores, cell-in-shell, cell nanoencapsulation, cell-surface engineering, interfacial self-assembly

Abstract: Single-cell nanoencapsulation, forming cell-in-shell structures, provides chemical tools for endowing living cells, in a programmed fashion, with exogenous properties that are neither innate nor naturally achievable, such as cascade organic-catalysis, UV filtration, and immunogenic shielding, as well as enhanced tolerance in vitro against lethal factors in real-life settings. Recent advances in the field make it possible to further fine-tune the physicochemical properties of the artificial shells encasing individual living cells, including on-demand degradability and re-configurability. Many different materials, other than polyelectrolytes, have been utilized as a cell-coating material with proper choice of synthetic strategies to broaden the potential applications of cell-in-shell structures to whole-cell catalysis and sensors, cell therapy, tissue engineering, probiotics packaging, and others. In addition to the conventional “one-time-only” chemical formation of cytoprotective, durable shells, an approach of autonomous, dynamic shellation also has recently been attempted to mimic naturally occurring sporulation process and to make the artificial shell actively responsive and dynamic. This progress report reviews recent development of synthetic strategies for formation of cell-in-shell structures along with advanced shell properties

acquired. Demonstrated applications, such as whole-cell biocatalysis and cell therapy, are discussed, followed by perspectives on the field of single-cell nanoencapsulation.

1. Introduction

Following the pioneering work of Möhwald,^[1] Diaspro,^[2] Lvov,^[3] and Tsukruk,^[4] the field of single-cell nanocoating and nanoencapsulation has skyrocketed. Early research humbly started with the use of fixed (i.e., dead) cells as a sacrificial template for the formation of hollow microcapsules,^[1] and rapidly advanced to the coating of live cells mainly based on the layer-by-layer (LbL; for the abbreviations used in this report, see **Table 1**) assembly of polyelectrolytes.^[2,3a] Since then, various synthetic strategies with different materials, other than polyelectrolytes, have been developed for forming cell-in-shell structures in a controlled fashion,^[3b,4b,5] and, particularly, the formation of ultrathin (< 100 nm), mechanically durable shells on living cells has provided chemical tools for manipulating cellular activities and metabolism at a single-cell level and also endowed the cells with enhanced tolerance against harmful stresses in vitro.^[6] The suggested applications of the cell-in-nano-nutshell structures^[7] (a.k.a. artificial spores^[8]) are diverse, ranging from cell therapy and regenerative medicine to biocatalysis and sustainable energy.

The explosive interest in single-cell nanoencapsulation has recently been growingly evident, indicated in part by the exponentially growing numbers of research papers and citations in the field (**Figure 1**). Since our first progress report in 2014,^[7] new synthetic strategies, beyond LbL, have been developed for cytocompatible nanoencapsulation of single cells, and many critical demonstrations have been made in the application areas. In this progress report, we discuss recent advances, mostly after 2013, in synthetic strategies to generate cell-in-shell structures, in conjunction with unprecedented shell properties made possible by the new

strategies. We also describe the applications demonstrated, including biocatalysis and cell therapy, followed by perspectives on the field of single-cell nanoencapsulation.

2. Progresses in Synthetic Strategies for “Cell-in-Shell” Structures

In this report, the synthetic strategies developed so far for cell nanoencapsulation can be classified as one of the following: “depositing-to” approach, “growing-from” approach, and interfacial reactions. However, some synthetic methods cannot be exclusively categorized. When proposed reaction mechanisms are not clearly “growing-from”, the methods are loosely classified as “depositing-to” approaches. In this classification, the LbL assembly is the “depositing-to” approach, where polyelectrolytes are deposited onto, not grown from, the substrate in most cases.

2.1. “Deposit-to” Approaches

In the “depositing-to” process, materials (i.e., small molecules, metals, nanoparticles, or polymers) and/or their aggregates and complexes—typically generated in the coating solution—are deposited directly to cell surfaces via physicochemical interactions. The shell thickness is either fixed per deposition (e.g., for LbL^[3b]) or varied depending on deposition time (e.g., for polydopamine^[9]). The deposition step is repeated to achieve desired shell thickness, if needed. The “grafting-to” approach in the area of polymer grafting can also be considered to be a “depositing-to” approach, although covalent linkages are typically formed between polymers (and small molecules) and the substrates to be grafted. Covalent “grafting-to” approaches for living cells, which usually involve the chemical modification of cell surfaces, are not discussed in this report.^[10]

The most intensively employed method in single-cell nanocoating is the LbL deposition of various polymers and nanomaterials onto cell surfaces (**Figure 2a**).^[1-4,11] In addition to the classical, electrostatics-based LbL deposition that might be cytotoxic because of positively charged polyelectrolytes, new strategies have been developed for more cytocompatible cell nanocoating, such as salting-out^[12] and hydrogen bonding-based approaches.^[4a,b,13] For example, Tsukruk and his co-workers formed tough, pH-responsive LbL shells on individual yeast cells, by cross-linking hydrogen-bonded layers composed of poly(*N*-vinylpyrrolidone) (PVPON) and amine-bearing poly(methacrylic acid) (PMAA-*co*-NH₂), to control cell function and metabolism without noticeable decrease in cell viability (**Figure 2b**).^[13a] The material scope for cell-surface engineering also has been widened, including silk fibroin (SF),^[12] halloysite nanotubes (**Figure 2c**),^[14] and small peptides.^[15]

Besides the LbL approach, recent strategic focus in single-cell nanoencapsulation has actively been made on material-independent film formation since our report on polydopamine (PD)-encapsulated yeast cells, which utilized the material-independent deposition of PD with dopamine as a precursor.^[16] The materials reported so far to be universal in film formation have all been polyphenols, such as tannic acid (TA) and pyrogallol (1,2,3-trihydroxybenzene, PG),^[17] and have been applied to cell nanoencapsulation to some extent. Direct deposition of polyphenolics onto cell surfaces has been achieved by optimizing the coating conditions to be compatible with living cells. Although high salt conditions (0.6 M NaCl), which are extremely hypertonic and hence not cytocompatible, were required for the universal coating of non-living substrates with PG,^[18] cell-surface coating was found to occur smoothly at pH 7.8 in an isotonic buffer, leading to the formation of cell-in-shell structures for both microbial and mammalian cells (human red blood cells (hRBCs) and HeLa cells) (**Figure 2d**).^[19] This depositing-to strategy proved extremely cytocompatible. For example, viability loss was not

noticeable after 4 h of PG coating on *Saccharomyces cerevisiae*. In comparison, the viability dropped to about 70% after 3 h of PD coating.^[16a]

Caruso and others reported that the uniform film of the supramolecular metal-TA coordination complex was formed on virtually any substrate, presumably owing to the surface-adhering property of TA.^[20] Among multivalent metals, ferric ion (Fe(III)) has intensively been used for catecholato-iron complex formation, inspired by the byssal cuticle of marine mussels that protects the byssal threads from abrasion,^[21] and has been applied to the formation of self-healing hydrogels^[22] and interfacial nanolayers^[23] along with thin film formation. The film deposition was achieved by either one-step deposition from a mixture of TA and Fe(III)^[20a,b] or LbL process involving the alternative deposition of TA and Fe(III).^[20c,d] The one-step immersive method is more favorable for cell-surface engineering, generating ~10-nm-thick films in less than 10 seconds, and does not involve laborious processes nor require toxic chemicals. Taking advantage of these beneficial characteristics, various microbial and mammalian cells have been cytocompatibly coated with the Fe(III)-TA metal-organic complex (Fe(III)-TA-MOC) (**Figure 2e**).^[24]

2.2. “Growing-from” Approaches

Recent years have witnessed an unforeseen interest in the growing-from strategies for cell nanoencapsulation (**Figure 3a**). An early example of the “growing-from” approach is the surface-induced hydrogelation of a naphthylated tripeptide, Nap-FFG (F: phenylalanine, G: glycine), on platelets,^[25] and the strategy of “grafting-from” polymerization (surface-initiated polymerization, SIP^[26]) has very recently been applied to living cells.

Controlled radical polymerization (CRP; e.g., atom-transfer radical polymerization (ATRP) and reversible addition-fragmentation chain-transfer polymerization (RAFT)) has particularly been used for cell-surface engineering, because of its advantageous characteristics including low concentration of radicals and low cross-reactivity of biological functional groups. The potential cytotoxicity of free radicals, generated from initiators and monomers during CRP, was minimized further in two reported approaches.^[27] In one approach, a radical-protective layer of PD-based macroinitiators was formed on yeast cell surfaces, and then a mild version of ATRP (activators regenerated by electron transfer ATRP, ARGET ATRP) in an aqueous solution was conducted (**Figure 3b**).^[27a] The radical-scavenging property of PD greatly increased the cell viability after SI-ARGET ATRP, forming “yeast-in-polymer” structures.

In the other approach, photoinduced electron-transfer RAFT (PET-RAFT) with visible light was utilized to grow high-density polymers from the initiators that were either covalently attached to (for yeast) or non-covalently inserted into (for Jurkat cells) the cell surface.^[27b] The reaction was extremely fast, minimizing its harmful effect on living cells. For example, SI-PET RAFT was performed for 5 min from 2-(butylthiocarbonothionyl)propionic acid-attached yeast cells with a 9:1 mixture of polyethylene glycol (PEG)-based acrylamide (PEGA-1k) and ω -azido PEGA-1k (PEGA-N₃-1k), and fluorescein diacetate (FDA) and flow cytometry analyses indicated the cell viability of over 90% (**Figure 3c**). The cytocompatibility of the method was astonishingly high, showing >90% viability even for Jurkat cells, which could not be coated cytocompatibly with the PD-based ATRP macroinitiator^[27a] due to its cytotoxicity to mammalian cells. The in situ polymerization of pyrrole from the surface of individual bacteria, such as *Shewanella oneidensis* MR-1, was also performed after electrostatic Fe(III) adsorption, and the polypyrrole (PPy) shell improved the conductivity of the cells while maintaining long-term cell viability (**Figure 3d**).^[28]

Cross-linked networks of polymer shells have been formed on mammalian cells by in situ radical polymerization (**Figure 3e**).^[29] Acryloylation was used to introduce vinyl groups on cell surfaces via *N*-acryloxysuccinimide (NAS)-mediated coupling, and the cross-linked polymer network was formed with acrylamide (AAm) as a monomer and glycerol dimethacrylate (GDMA) as a cross-linker. Cell viability after encapsulation was strikingly high, considering the polymerization time; after 2 h of polymerization, the cell viability for HeLa cells was about 80%. Another strategy for coating individual cells with cross-linked hydrogels was developed based on horseradish peroxidase (HRP)-catalyzed oxidative coupling of phenol (Ph) derivatives in the presence of hydrogen peroxide (H₂O₂) (**Figure 3f**).^[30] HRP was immobilized onto cell surfaces by using an anchoring molecule,^[31] and various polymers having a Ph moiety, such as alginate (ALG), hyaluronic acid (HA), gelatin, and poly(vinyl alcohol), were cross-linked to form a hydrogel sheath for living cells including mouse embryonic fibroblast cell line S: Sandos inbred mice; T: 6-thioguanine resistant; O: ouabain resistant (STO) and human hepatoma HepG2 cells.^[30a] The trypan blue exclusion test indicated that the encapsulation process had no adverse effects to the cells, and the viability was about 90% after 30 min of cross-linking reaction. The strategy was also applied to the identification of H₂O₂-secreting cells.^[30b]

Another powerful “growing-from” strategy involves the cell surface-induced formation of metal-organic framework (MOF) crystals.^[32a,b] The mechanistic studies suggest that the cell surfaces (biomolecule-rich cell membranes and walls) concentrate MOF precursors, which provides an interface for MOF crystallization.^[32c,d] In this sense, the method resembles the bioinspired mineralization of ionic compounds in single-cell encapsulation (the bioinspired silicification is considered to be “depositing-to”^[33]).^[34] Specifically, *S. cerevisiae* or *Micrococcus luteus* were dispersed in an aqueous solution of 2-methylimidazole, and an aqueous solution of zinc acetate (Zn(OAc)₂) was added. The 10 min of reaction formed a

cytoprotective, porous zeolitic imidazole framework-8 (ZIF-8) shell (thickness: ~100 nm) on individual microbial cells without noticeable decrease in cell viability (**Figure 3g**). They also immobilized β -galactosidase onto yeast cells before ZIF-8 shell formation to further enhance the cell survival in an oligotrophic environment.^[32e] After 7 days of incubation in the nutrient-deficient media containing lactose (not glucose), most native yeast cells were dead, but the cell viability of encapsulated cells dropped only about 30% because of β -galactosidase-catalyzed conversion of lactose into glucose and galactose.

2.3. Interfacial Reactions

Certain organisms, such as bacteria, fungi, ciliates, and even invertebrates, enter cryptobiotic states in response to harmful external stresses to prolong survival. For example, *Bacillus subtilis* forms a robust hierarchical shell, transforming themselves into bacterial endospores.^[35] It could be envisioned that, in the laboratory setting, cells are programmed to sense harmful molecular factors in the environments, and release the “catching” components to form neutralized pericellular layers with the harmful factors. Ideally, this interfacial shell formation could provide long-term protection and preservation as well as counteract the harmful attacks, not to mention that the process is autonomous and self-regulated.

Supramolecular self-assembly across interfaces in two immiscible phases (“biphasic interfacial supramolecular self-assembly”, BI-SMSA^[23a]) involves contact-based self-assembly at the interface of two immiscible phases, typically oil and water, each of which contains a reacting component (**Figure 4a**). For example, the structural motif of MOFs has intensively been utilized to form hollow capsules^[36a,b] and fibers.^[36c] Host-guest supramolecular chemistry^[37] and polyelectrolyte complex formation^[38] were also utilized for BI-SMSA. The first BI-SMSA attempt for cell-surface engineering was made with dead-cell

scaffolds,^[39] as dead red blood cells (RBCs), which had been used as sacrificial LbL templates for the formation of hollow capsules.^[1] Pure cell wall structures of yeast, obtained by treatment of hot water and methanol, acted as reservoirs for metal ions (Zn(II) or Cu(II)), and BI-SMSA led to the formation of MOF crystal layers outside and inside of the cell wall (ZIF-8 or CuBTC (BTC: 1,3,5-benzenetricarboxylate)) (**Figure 4b**). The BI-SMSA strategy has further advanced to the autonomous formation of durable shells around individual living yeast cells (**Figure 4c**).^[23a] The cells were pre-fed with Fe(III) under cytocompatible conditions and then exposed to TA in solution. The passive efflux of Fe(III) to the solution made its contact with TA at the pericellular space, leading to the formation of durable Fe(III)-TA-MOC shells. The shell formation was rapid, and the Fe(III)-TA-MOC shells formed only on the Fe(III)-fed cells in mixtures of Fe(III)-fed cells and Fe(III)-non-fed cells, without any promiscuous reactions between two types of cells. This result suggests the possibility of developing active strategies involving cells as reservoirs for the release of molecules that react immediately with other components in the extracellular milieu to form stable and homogeneous nanocoatings.

3. Advances in Nanoshell Properties

Strategic advances in cell-in-shell structures were naturally translated into the emergence of new shell properties that could not have been achieved previously. In short, the shells were more dynamic and responsive compared with first-generation shells. The shells were either degradable or re-configurable in response to changes in environmental conditions.

3.1. On-Demand Degradability: Chemical Sporulation and Germination

One of the advances made during the past several years is the fabrication of degradable shells, which differ from breakable shells. All shells fabricated so far are breakable in a sense; the shells cannot withstand the division force of the cells inside and are broken apart eventually when the cells divide. The “degradable” shells are broken apart in a chemically controlled fashion in response to external stimuli or inducers. This degradation on-demand is highly beneficial in applications that require fully functional cells, such as whole-cell biosensors and cell therapies.^[40] The cells should be preserved and stored safely against harmful stresses in daily-life or laboratory settings and liberated from the encasing shells for proper functioning at the desired time and space. In other words, the cells are to be sheathed and made strong by the shells (chemical sporulation) and released for functional work (chemical germination). In this sense, this type of “cell-in-shell” structures are called micrometric Iron Men.^[6]

The shell should be chemically robust for cytoprotection and also degradable under cytocompatible conditions, which may seem contradictory from a chemistry point of view. One strategy to chemical sporulation and germination is based on metal-ligand coordination complexes, which could, in principle, be disassembled by relatively mild stimuli, such as changes in pH or chelating ligands. The first demonstration of chemical sporulation and germination used Fe(III)-TA-MOC as a shell scaffold (**Figure 5a**).^[24] After treatment of HCl (20 mM, 90 min), the log(CFU mL⁻¹) value (CFU: colony-forming unit) of yeast@[Fe(III)-TA-MOC] dramatically increased from 4.47 to 6.91, which was similar to that for native yeast, 7.01.^[24a] This result indicated that the cell-division activity, suppressed by the Fe(III)-TA-MOC shell, was restored on demand. The Fe(III)-TA-MOC shell on mammalian cells was also degraded controllably.^[24b] For example, while the encapsulated HeLa cells maintained their spherical shape without any observable attachment to the culture surface even after 96 h of culture, they adhered to and grew on the culture flask after 96 h of incubation in Dulbecco’s modified Eagle’s medium containing 0.5 mM ethylenediaminetetraacetic acid

(EDTA). EDTA was also used to degrade the ZIF-8 MOF shell and induce the cell growth and germination states (**Figure 5b**).^[32a]

Degradable polymer nanoshells have recently been developed.^[41] Thiol-exchange reactions were delicately designed to cross-link LbL layers in situ, generating a disulfide-linked polyelectrolyte multilayer (PEM) that was broken into thiols by glutathione (GSH) (**Figure 5c**).^[41a] The combination of thiol-maleimide coupling and retro-Michael-type addition reactions was also utilized to degrade the cross-linked shell with GSH (**Figure 5d**).^[41b] To provide the cells with extracellular matrix (ECM)-mimetic, biocompatible environments,^[42] gelatin derivatives were used for cell coating, and the cross-linking was made between a layer of gelatin type B (GB)-4arm-PEG-thiol and 8arm-PEG-maleimide. Most of the encapsulated HeLa cells could adhere and spread on a surface after 48 h of cultivation with GSH (10 mM), indicating shell degradation.

Another approach to chemical sporulation and germination was the use of biodegradable materials as nanoshell components. Structural transition of water-soluble random-coil SF to water-insoluble β -sheet SF was induced on the cell surface by the salting-out process of a kosmotropic phosphate buffer, and the SF nanoshell (~10 nm thick) was generated without compromising cell viability (up to 97% for *S. cerevisiae*).^[12a] Of great interest is that the SF shell was digested by the cell during its active growth, releasing the cell with full functionality from the temporarily protective shell (**Figure 5e**). SF was further modified with poly-L-lysine (PLL), poly-L-glutamic acid (PGA), and PEG with different grafting densities and architectures to vary the physicochemical properties of SF shells, such as robustness and degradation profiles.^[12b] This digestion-based shell degradation actively uses the inherent biochemical activities of cells, which are mechanistically different from external stimuli-induced shell degradation; the degradation timing, in principle, can be set under well-defined

conditions, with proper selection of materials and assembling parameters, presumably even in vivo. It may also be possible that the cells, upon the activation by an external inducer, chew the shells apart for on-demand exposure.

3.2. Re-Configurability

Cell nanoencapsulation does not completely shut down but seemingly retards cellular activities,^[16b,43] and the encapsulated cells eventually grow, divide, and proliferate under culture conditions by breaking the shells. Although cells can be stored and protected in the non-culture conditions for future use, it would also be beneficial in the applications to establish a strategy that enables “continuous” shellation during division and proliferation. For example, in the biocatalysis application, metabolic activities are commonly required for catalytic reactions, and cell division would be inevitable, ultimately leading to the uncontrolled breakage of cytoprotective shells and undesired cell death under catalysis-reaction conditions. The BI-SMSA-based autonomous shellation^[23a] would be one of the promising strategies to pursue in the continuous formation of cytoprotective shells.

A strategy of “self-repairing” nanoshells has been proposed based on self-assembly of nanomaterials on cell surfaces.^[44] Specifically, nanoaggregates of gold nanoparticles (AuNPs) and an amino acid, such as L-cysteine (AuNP-L-cysteine aggregates)^[45] acted as a sol precursor for a uniform shell (thickness: 160 nm for yeast), and the excess aggregates present in the solution contributed to the continuous shell formation in the division cycle (**Figure 5f**). It is noteworthy that other materials, such as AuNP@polymer, did not show the self-repairing property.

4. Demonstrated Applications

The cytoprotective capabilities of cell-in-shell structures promise the functional utilization of cells inside the shells in various technologically important applications, and recent years have witnessed some promising demonstrations (**Table 2**). The cytoprotective shells also can be have been functionalized further to meet the requirements of some applications. For example, the magnetized cells could be spatially manipulated, concentrated, and isolated en masse, beneficial in the facile recycling of biocatalytic cells and localization of biosensing cells in a device, in addition to tissue-engineering applications.^[46,47]

4.1. Whole-Cell Biocatalysis

Much work has been done with photosynthetic microbes, which are considered to be the most promising sustainable source of biomass, to maximize their photochemical efficiency under normal, daily-life conditions that adverse biocatalytic activities. The underlying idea was to protect the cells from excessive sunlight, which generally causes photoinhibition and cell death, by forming cell-in-shell structures; UV radiation is also lethal, and even its natural level in the environment can significantly affect the enzymatic activities and destroy the photosystem II (PSII) structure.^[48]

The first attempt in this direction was made in 2013 by Tang *et al.*, who encapsulated unicellular cyanobacteria, *Synechocystis* sp. strain PCC 6803, within a silica shell, formed by a combination of LbL and bioinspired silicification,^[33b] and demonstrated that the silica shell alleviated high-light-induced photoinhibition (**Figure 6a**).^[49a] They also used UV-filtering CeO₂ (ceria) nanoparticles to protect *Chlorella pyrenoidosa* from UV irradiation:^[49b] the maximum quantum yield of PSII (F_v/F_m) stayed at about 76% for the ceria-decorated *C.*

prenoidosa even after 24 h of continuous UV-B radiation, while native *C. prenoidosa* lost about 86% of their photosynthetic activity under the same conditions. Accordingly, the O₂ evolution from native *C. prenoidosa* stopped after 6 h of UV-B irradiation, but *Chlorella*@CeO₂ kept 46% of the original activity. Su and co-workers also formed a bilayer shell of AuNP-L-cysteine and SiO₂ nanoparticles around cyanobacteria, *Synechococcus* 7942, for use as a photosynthetic bioreactor.^[49c] It was reported that, even after 20 days of high-light irradiation (3000 Lx), the photosynthetic activity of oxygen production was 180% of the initial activity of the encapsulated cells, but that of native cells became almost undetectable. In addition, the double-layered shell effectively protected the cells inside from pH fluctuation (by buffering effect of L-cysteine) and UV irradiation. Additionally, Tang *et al.* delicately designed a H₂-producing biocatalytic system that was sustainable under aerobic conditions (**Figure 6b**).^[49d] Hydrogenase, which produces H₂ from H⁺, loses its function in the presence of O₂, but its activity was made active under natural aerobic environment by forming self-aggregates of *Chlorella*@SiO₂. The twofold enhanced H₂ production also has been reported with TiO₂-encapsulated *Chlamydomonas reinhardtii* under sulfur-deprived conditions during a 5-day period.^[49e]

In addition to solar-to-chemical energy conversion, biocatalytic organic transformations have been investigated with cell-in-shell structures. Su *et al.* utilized the strategy of PD nanoencapsulation^[16a] for *Rhodotorula glutinis*, which produces chiral alcohol with high enantiomeric excess.^[50a] The (*S*)-1-phenylethanol productivity from acetophenone was found to be 5 times higher for the encapsulated cells compared with native cells, presumably because of the electron transfer capability of PD shells (**Figure 6c**). This example illustrates the shell-mediated control of cellular activities. The reusability was also greatly enhanced by the cytoprotective PD shell that was magnetically functionalized further; while the reaction yield sharply dropped to 7.9% after five batches for native cells, it decreased slightly to 67.3%

in the case of encapsulated cells. They also reported that hybrid shells additionally showed effective protection of cells during the bioreduction. For example, *R. glutinis* encapsulated within a PD/TiO₂ hybrid shell presented a yield as high as 70.9% after 24 h of reaction with UV irradiation, but native cells displayed a low yield of 28.8% under the same reaction conditions. In the same line, *Gordonia* sp. WQ-01A was coated with AuNP-L-lysine/TiO₂ hybrid to enhance its desulfurizing activity (e.g., sulfur removal from dibenzothiophene).^[50b] On the other hand, oil-degrading *Alcanivorax borkumensis* was magnetized for potential application to bioreactor-based oil-processing devices.^[46a]

Cell-in-shell structures have also been used as a Pickering interfacial biocatalyst.^[51]

Individual *Alcaligenes faecalis* ATCC8750 cells were coated with calcium phosphate, and the stable Pickering emulsion was formed in the toluene-water biphasic system by optimizing the hydrophilic/phobic balance of the shell with sodium monododecyl phosphate. With the bioconversion of (*R,S*)-mandelonitrile to *R*-(-)-mandelic acid as a model, the specific activity was found to be 3.88 and 18.41 times higher than that for the bacteria in SiO₂-particle-stabilized Pickering emulsions and for the bacteria in ALG beads, respectively (**Figure 6d**). It is noteworthy that the bacteria were protected from organic-solvent stresses during reaction and recycling. High conversion efficiency above 80% was observed even after 30 cycles, and the stereoselectivity remained almost constant.

PPy-encapsulated *Shewanella oneidensis* MR-1 cells have been utilized as an anode in microbial fuel cells (MFCs) that harness the metabolism of exoelectrogenic *S. oneidensis* to harvest electricity from lactate.^[28] The use of PPy-encapsulated bacteria greatly enhanced the direct contact-based extracellular electron transfer (EET) for at least 10 days without any significant loss of cell viability. For example, the charge transfer resistance (R_{ct}) significantly decreased to ~45.6 Ω from ~1106.9 Ω (for native bacteria) after shell formation; the

maximum power density was also 14.1 times higher (147.9 vs. 9.8 $\mu\text{W cm}^{-2}$) (**Figure 6e**). It was suggested that the affinitive mechanical contact with *c*-type cytochromes on the outer membrane of the bacteria, responsible for electron transfer from the cell to an anode, was enhanced by the conducting PPy shell.

4.2. Cell Therapy

Successful demonstrations in whole-cell biocatalysis, described in the previous section, benefit highly from the durable shells that protect the biocatalytic cells inside from harmful external factors during their functional activities.^[6] The cytoprotectability of the shells also has been utilized to prolong the survival and increase the efficacy of mesenchymal stem cells (MSCs) in their intravenous administration for in vivo cell therapy.^[15] The nanocoated MSCs showed the increased blood circulation lifetime, against sheer stress in the blood stream, and the enhanced stem cell recruitment to injured tissues in an in vivo model (**Figure 7a**).

Although these previous examples show that the artificial-spore structures have great potential for their practical realization in the applications heavily requiring the cytoprotection capability, some industrial applications critically rely on biochemical interactions at cell surfaces (i.e., juxtacrine interactions) and subsequent signal transduction, at least for desired biological functions. For example, in the natural killer (NK)-cell infusion cancer therapy, the antigen-receptor binding must occur between NK cells and tumorous cells for eradication of the tumorous cells.^[52] However, it is not an easy task to preserve this type of biochemical recognition while protecting the cells with artificial shells for prolonged and sustained cell viability. Stimuli-responsive degradation of cytoprotective shells^[24a-c,32a] may be one of the strategic approaches for restoring cellular recognition and activities after temporal protection in vitro, but the chemical methods developed, such as pH changes and EDTA addition, cannot

be applied directly to in vivo systems. Therefore, the application of cell-in-shell structures to cell therapy and related nanomedicinal areas has been limited so far. Very recently, it has been reported that the juxtacrine interactions and cytokine secretion, crucial for cell-therapeutic applications, are undisturbed even after durable-shell formation, although detailed working mechanisms remain to be seen.^[53] Jurkat cells, a human leukemic T-cell line, as a model for therapeutic cells, were coated with TiO₂ by (RKK)₄D₈-induced TiO₂ formation (R: arginine, K: lysine, D: aspartic acid).^[54] The antigens, such as CD3 and CD28, were accessible for binding, and the stimulated Jurkat cells secreted interleukin-2 (IL-2) properly (**Figure 7b**), showing that cell-in-shell structures could be applied to cell therapy with proper selection of coating materials and synthetic strategies.

Another direct application of cell-in-shell structures is found in the development of universal blood.^[55] RBCs have been encapsulated within a PD shell for sheltering antigenic epitopes.^[56] RBC agglutination with its anti-type antisera was inhibited by the PD shell, and the physicochemical properties, such as osmotic fragility, deformability, surface charge, and hydrophobicity, were not noticeably changed by shell formation. Of more importance is no significant difference in the in vivo survival profile of RBC@PD during the lifespan of the transfused RBCs to mice (**Figure 7c**). Fe(III)-TA-MOC and pyrogallol coatings have also been applied to RBCs for antigen shielding.^[19,24d]

4.3. Probiotics

Recent years have witnessed some progress in the cytoprotection of individual probiotics, which would be one of the simplest applications of artificial spores but still have a great impact on human welfare. The low bioavailability of probiotics has been one of the limitations in the clinical applications, because of the loss in viability during gastrointestinal

(GI) transit due to low pH, bile salts, enzymatic attack, and others. It was suggested that the physiologically active concentration of probiotics in the gut be 10^6 - 10^7 CFU (g intestinal contents)⁻¹.^[57] To meet the market demand, recent effort has been made to coat individual probiotic microbes, mainly by LbL techniques, to protect them in the GI tract, especially in the stomach, and to promote adhesion and growth in the desired sites.^[58] For example, *Lactobacillus acidophilus* was coated with the PEMs of chitosan (CHI) and carboxymethyl cellulose,^[58a] *Saccharomyces boulardii* with those of CHI and dextran sulfate,^[58b] and *Bacillus coagulans* with those of CHI and ALG.^[58c] In all cases, the increased CFU values in the stimulated gastric fluid (SGF, pH 2) were observed for LbL-coated probiotics. In the latter, in vivo experimentation with mice has also been performed to show the enhanced survival and delivery of probiotics in the GI tract (**Figure 7d**).^[58c] A block-copolymer of pluronic and poly(acrylic acid) has also been used with CHI for LbL coating of *Lactobacillus debrueckii* subsp. *bulgaricus*,^[58d] and a combination of CHI and sulfated β -glucan for *L. acidophilus*.^[58e] In all the examples above, CHI, a random linear copolymer of (1-4)-*N*-acetyl-D-glucosamine and (1-4)-D-glucosamine produced by deacetylation of chitin, was used as a cationic polyelectrolyte because the choice of cationic biopolymers is extremely limited compared with anionic biopolymers. However, the pK_a of CHI is about 6.4, and it is rarely soluble at neutral pH; it cannot be applied to pH-sensitive cells in cell nanoencapsulation.^[59a] In addition, CHI is antimicrobial, killing bacteria, yeast, and fungi.^[59b] In this sense, it is highly desired to obtain highly biocompatible polycations, for example by derivatizing nature-derived biopolymers.^[60]

4.4. Other Applications

Cytoprotective and, simultaneously, bioactive shell formation has been attempted for advanced vaccine development; live vaccine-strain *Bacillus Calmette-Guérin* (BCG) was

coated with CHI and polyriboinosinic acid-polyribocytidylic acid (poly(I:C)), a strong inducer of cell-mediated immunity, to enhance the immunogenicity of the BCG vaccine against tuberculosis.^[61] On the other hand, cancer-cell-targeting shell formation, which kills cancer cells, has also been reported, where the pericellular hydrogel nanonets precluded the passing-through of materials (and even small molecules)^[62a] or the mineral-based shell components disrupted the integrity of cell membranes.^[62b]

5. Perspectives

The field of single-cell nanoencapsulation has boomed during the last several years. Many different materials have successfully been employed as a cell-coating material, and new shell-properties have been extracted from their innate physicochemical properties and integrated synergistically with biological functions of cells inside. For example, natural biopolymers have been suggested as more biofriendly and functional coating materials over traditional synthetic polymers.^[12,63] Many attempts also have been made for the realization of cell-in-shell structures in the application sectors, such as biocatalysis and cell therapy.

Despite the eye-catching and promising reports, there is still much to improve in the aspect of shell properties, which would be made possible by development of synthetic strategies with new materials. For example, the use of manganese dioxide (MnO_2) as a shell material in a very recent report conferred non-biological, exogenous catalytic capability on the encased cells (**Figure 8a**).^[64] In addition to GSH-induced shell-degradation, the MnO_2 shell possessed multienzyme-like activities of superoxide dismutase and catalase and protected the cells from toxic chemicals, such as H_2O_2 . Another important shell property to achieve, in addition to cytoprotection capability, would be the chemical controllability of cell aggregation and

coagulation, which is critically beneficial to applications, such as 3-dimensional (3D) cell printing (**Figure 8b**).^[65]

On the other hand, new advances in the shell properties are suggested to be tailor-made, and the choice of coating materials and synthetic strategies be decided based on the applications in mind. In the area of biocatalysis, the shell does not need to be degraded but should rather be durable and protective enough to maintain the desired catalytic activities of microbes against harmful stresses in the extended periods of time. Considering that many organic transformations proceed in organic solvents, the durable shell should be designed to protect the microbes inside from organic solvents and toxic chemicals. This should also apply to mammalian cells, because some cell-manipulation procedures require the use of oils and other chemicals.^[66] In cell-therapy applications, shell cytocompatibility is critical, but, more importantly, the preservation of juxtacrine interactions (e.g., antigen-antibody interaction) and chemical diffusion *in vivo* is a prerequisite to proper functions of therapeutic cells. The shell could be degraded in a programmed fashion inside the body, or it could be designed to be adaptable to the environment and/or porous enough to maintain the juxtacrine recognition and signaling^[53,67]. In regenerative medicine, it would be highly desirable that biochemical and mechanical properties of artificial shells control the differentiation pathway of the encapsulated cells or tune their attachment to biomaterials or to specific anatomic locations *in vivo*.

Shell properties will ideally advance further to the point of mimicking natural processes of sporulation, generating dynamic, adaptive, and self-healing shells on single cells. In addition to the crytobiotic states, nature additionally provides an inspiring examples in this direction, such as zinc spark-induced hardening of egg zona pellucida that prevents polyspermy.^[68] The synthetic strategies demonstrated so far heavily rely on the static states of cells to coat, which

means that the cells are considered crudely to be “dead” objects during the process of shell formation. In this philosophical approach, the cytocompatibility of materials and strategies is only deterministic to the successful formation of cell-in-shell structures. On the other hand, future progress would be found in the utilization of dynamic states of cells, which is more natural and biological. The cells themselves could sense and respond to the sporadic fluctuation of outside in vitro (and in vivo) conditions, and form or degrade the shells autonomously. The promising finding in a recent report showed that yeast cells respond to the presence of TA in the medium and form the pericellular Fe(III)-TA-MOC shells.^[23a] The autonomous shell formation and degradation would be extremely beneficial in many application areas aforementioned, not to mention the huge leap in chemical manipulability of cellular metabolism at the single-cell level.

Regarding the cell types, chemical applicability is still limited to the microbial cells encased within durable cell walls, although some cytocompatible strategies have been developed and reported for mammalian cells. Although the encapsulated microbes provide useful applications including whole-cell biocatalysis, more applications can be envisioned with the cytoprotective and cytocompatible coating of mammalian cells, such as cell therapy^[15] and stem cell-driven tissue growth (**Figure 8c**).^[63] Previous reports indicate that the viability of mammalian cells is highly dependent upon cell types when coated with a given material. Therefore, a specific material and synthetic strategy might be needed for a specific cell type to sustain its viability during and after cell-in-shell coating. In addition, more work will be necessary to practicalize the coating conditions for large-scale production for various biotechnological applications, by reducing the coating time and finding more green, milder, and economically more attractive processes.

The potential of single-cell nanoencapsulation has been demonstrated during the past years: many different materials have been used; new synthetic strategies developed; advanced shell properties acquired; many promising applications shown. It is envisioned that the field of single-cell nanoencapsulation will advance further to meet the practical requirements of industrial applications as well as providing 3D biochemical systems for fundamental studies in biochemistry and biology. Hierarchical structures, composed of artificial spores and (sub)milli-capsules,^[69] would also benefit to this end.

Acknowledgements

This work was supported by the Basic Science Research Program through the National Research Foundation of Korea (NRF) funded by the Ministry of Science, ICT & Future Planning (MSIP 2012R1A3A2026403). J.F.M. acknowledges the European Research Council grant agreement ERC-2014-ADG-669858 for project ATLAS.

References

- [1] a) S. Leporatti, A. Voigt, R. Mitlöhner, G. Sukhorukov, E. Donath, H. Möhwald, *Langmuir* **2000**, *16*, 4059; b) B. Neu, A. Voigt, R. Mitlöhner, S. Leporatti, C. Y. Gao, E. Donath, H. Kieseewetter, H. Möhwald, H. J. Meiselman, H. Bäumlner, *J. Microencapsul.* **2001**, *18*, 385; c) E. Donath, S. Moya, B. Neu, G. B. Sukhorukov, R. Georgieva, A. Voigt, H. Bäumlner, H. Kieseewetter, H. Möhwald, *Chem. Eur. J.* **2002**, *8*, 5481.
- [2] A. Diaspro, D. Silvano, S. Krol, O. Cavalleri, A. Gliozzi, *Langmuir* **2002**, *18*, 5047.
- [3] a) H. Ai, M. Fang, S. A. Jones, Y. M. Lvov, *Biomacromolecules* **2002**, *3*, 560; b) R. F. Fakhrullin, Y. M. Lvov, *ACS Nano* **2012**, *6*, 4557.
- [4] a) V. Kozlovskaya, S. Harbaugh, I. Drachuk, O. Shchepelina, N. Kelley-Loughnane, M. Stone, V. V. Tsukruk, *Soft Matter* **2011**, *7*, 2364; b) J. L. Carter, I. Drachuk, S. Harbaugh,

- N. Kelley-Loughnane, M. Stone, V. V. Tsukruk, *Macromol. Biosci.* **2011**, *11*, 1244; c) I. Drachuk, M. K. Gupta, V. V. Tsukruk, *Adv. Funct. Mater.* **2013**, *23*, 4437.
- [5] R. F. Fakhrullin, A. I. Zamaleeva, R. T. Minullina, S. A. Konnova, V. N. Paunov, *Chem. Soc. Rev.* **2012**, *41*, 4189.
- [6] a) J. H. Park, D. Hong, J. Lee, I. S. Choi, *Acc. Chem. Res.* **2016**, *49*, 792; b) K. Bourzac, *Chem. Eng. News* **2016**, *94(43)*, 23.
- [7] J. H. Park, S. H. Yang, J. Lee, E. H. Ko, D. Hong, I. S. Choi, *Adv. Mater.* **2014**, *26*, 2001.
- [8] a) D. Hong, E. H. Ko, I. S. Choi, in *Cell Surface Engineering: Fabrication of Functional Nanoshells* (Eds: R. F. Fakhrullin, I. S. Choi, Y. Lvov), Royal Society of Chemistry, Cambridge, UK **2014**, pp. 142-161; b) S. H. Yang, D. Hong, J. Lee, E. H. Ko, I. S. Choi, *Small* **2013**, *9*, 178; c) D. Hong, M. Park, S. H. Yang, J. Lee, Y.-G. Kim, I. S. Choi, *Trends Biotechnol.* **2013**, *31*, 442.
- [9] H. Lee, S. M. Dellatore, W. M. Miller, P. B. Messersmith, *Science* **2007**, *318*, 426.
- [10] a) B. Kellam, P. A. De Bank, K. M. Shakesheff, *Chem. Soc. Rev.* **2003**, *32*, 327; b) C. A. Custódio, J. F. Mano, *ChemNanoMat* **2016**, *2*, 376; c) B. G. Mathapa, V. N. Paunov, *Biomater. Sci.* **2014**, *2*, 212; d) J. A. Giraldo, R. D. Molano, H. R. Rengifo, C. Fotino, K. M. Cattás-Asfura, A. Pileggi, C. L. Stabler, *Acta Biomater.* **2017**, *49*, 272; e) H. R. Rengifo, J. A. Giraldo, I. Labrada, C. L. Stabler, *Adv. Healthcare Mater.* **2014**, *3*, 1061; f) A. A. Tomei, V. Manzoli, C. A. Fraker, J. Giraldo, D. Velluto, M. Najjar, A. Pileggi, R. D. Molano, C. Ricordi, C. L. Stabler, J. A. Hubbell, *Proc. Natl. Acad. Sci. USA* **2014**, *111*, 10514.
- [11] a) M. Matsusaki, M. Akashi, in *Cell Surface Engineering: Fabrication of Functional Nanoshells* (Eds: R. F. Fakhrullin, I. S. Choi, Y. Lvov), Royal Society of Chemistry, Cambridge, UK **2014**, pp. 216-239; b) M. Matsusaki, H. Ajiro, T. Kida, T. Serizawa, M. Akashi, *Adv. Mater.* **2012**, *24*, 454; c) M. B. Oliveira, J. Hatami, J. F. Mano, *Chem. Asian J.*

- 2016**, *11*, 1753; d) J. J. Richardson, J. Cui, M. Björnmalm, J. A. Braunger, H. Ejima, F. Caruso, *Chem. Rev.* **2016**, *116*, 14828.
- [12] a) I. Drachuk, O. Shchepelina, S. Harbaugh, N. Kelley-Loughnane, M. Stone, V. V. Tsukruk, *Small* **2013**, *9*, 3128; b) I. Drachuk, R. Calabrese, S. Harbaugh, N. Kelley-Loughnane, D. L. Kaplan, Morley Stone, V. V. Tsukruk, *ACS Nano* **2015**, *9*, 1219.
- [13] a) I. Drachuk, O. Shchepelina, M. Lisunova, S. Harbaugh, N. Kelley-Loughnane, M. Stone, V. V. Tsukruk, *ACS Nano* **2012**, *6*, 4266; b) V. Kozlovskaya, O. Zavgorodnya, Y. Chen, K. Ellis, H. M. Tse, W. Cui, J. A. Thompson, E. Kharlampieva, *Adv. Funct. Mater.* **2012**, *22*, 3389; c) V. Kozlovskaya, B. Xue, W. Lei, L. E. Padgett, H. M. Tse, E. Kharlampieva, *Adv. Healthcare Mater.* **2015**, *4*, 686; d) D. Pham-Hua, L. E. Padgett, B. Xue, B. Anderson, M. Zeiger, J. M. Barra, M. Bethea, C. S. Hunter, V. Kozlovskaya, E. Kharlampieva, H. M. Tse, *Biomaterials* **2017**, *128*, 19.
- [14] S. A. Konnova, I. R. Sharlpova, T. A. Demina, Y. N. Osin, D. R. Yarullina, O. N. Ilinskaya, Y. M. Lvov, R. F. Fakhrullin, *Chem. Commun.* **2013**, *49*, 4208.
- [15] D. Choi, H. Lee, H.-B. Kim, M. Yang, J. Heo, Y. Won, S. S. Jang, J. K. Park, Y. Son, T. I. Oh, E. A. Lee, J. Hong, *Chem. Mater.* **2017**, *29*, 2055.
- [16] a) S. H. Yang, S. M. Kang, K.-B. Lee, T. D. Chung, H. Lee, I. S. Choi, *J. Am. Chem. Soc.* **2011**, *133*, 2795; b) D. Hong, H. Lee, E. H. Ko, J. Lee, H. Cho, M. Park, S. H. Yang, I. S. Choi, *Chem. Sci.* **2015**, *6*, 203; c) B. J. Kim, T. Park, H. C. Moon, S.-Y. Park, D. Hong, E. H. Ko, J. Y. Kim, J. W. Hong, S. W. Han, Y.-G. Kim, I. S. Choi, *Angew. Chem. Int. Ed.* **2014**, *53*, 14443; d) B. J. Kim, T. Park, S.-Y. Park, S. W. Han, H.-S. Lee, Y.-G. Kim, I. S. Choi, *Chem. Asian J.* **2015**, *10*, 2130.
- [17] H. Ejima, J. J. Richardson, F. Caruso, *Nano Today* **2017**, *12*, 136.
- [18] T. S. Sileika, D. G. Barrett, R. Zhang, K. H. A. Lau, P. B. Messersmith, *Angew. Chem. Int. Ed.* **2013**, *52*, 10766.

- [19] J. Y. Kim, H. Lee, T. Park, J. Park, M.-H. Kim, H. Cho, W. Youn, S. M. Kang, I. S. Choi, *Chem. Asian J.* **2016**, *11*, 3183.
- [20] a) H. Ejima, J. J. Richardson, K. Liang, J. P. Best, M. P. van Koevorden, G. K. Such, J. W. Cui, F. Caruso, *Science* **2013**, *341*, 154; b) J. Guo, Y. Ping, H. Ejima, K. Alt, M. Meissner, J. J. Richardson, Y. Yan, K. Peter, D. von Elverfeldt, C. E. Hagemeyer, F. Caruso, *Angew. Chem. Int. Ed.* **2014**, *53*, 5546; c) S. Kim, D. S. Kim, S. M. Kang, *Chem. Asian J.* **2014**, *9*, 63; d) M. A. Rahim, H. Ejima, K. L. Cho, K. Kempe, M. Müllner, J. P. Best, F. Caruso, *Chem. Mater.* **2014**, *26*, 1645.
- [21] a) M. J. Sever, J. T. Weisser, J. Monahan, S. Srinivasan, J. J. Wilker, *Angew. Chem. Int. Ed.* **2004**, *43*, 448; b) M. J. Harrington, A. Masic, N. Holten-Andersen, J. H. Waite, P. Fratzl, *Science* **2010**, *328*, 216.
- [22] a) N. Holten-Andersen, M. J. Harrington, H. Birkedal, B. P. Lee, P. B. Messersmith, K. Y. Lee, J. H. Waite, *Proc. Natl. Acad. Sci. USA* **2011**, *108*, 2651; b) M. Krogsgaard, A. Andersen, H. Birkedal, *Chem. Commun.* **2014**, *50*, 13278; c) S. Azevedo, A. M. S. Costa, A. Andersen, I. S. Choi, H. Birkedal, J. F. Mano, *Adv. Mater.* **2017**, *29*, 1700759; d) J. Sedó, J. Saiz-Poseu, F. Busqué, D. Ruiz-Molina, *Adv. Mater.* **2013**, *25*, 653.
- [23] a) B. J. Kim, S. Han, K.-B. Lee, I. S. Choi, *Adv. Mater.* **2017**, *29*, 1700784; b) M. A. Rahim, M. Björnmalm, N. Bertleff-Zieschang, Q. Besford, S. Mettu, T. Suma, M. Faria, F. Caruso, *Adv. Mater.* **2017**, *29*, 1606717.
- [24] a) J. H. Park, K. Kim, J. Lee, J. Y. Choi, D. Hong, S. H. Yang, F. Caruso, Y. Lee, I. S. Choi, *Angew. Chem. Int. Ed.* **2014**, *53*, 12420; b) J. Lee, H. Cho, J. Choi, D. Hong, D. Kim, J. H. Park, S. H. Yang, I. S. Choi, *Nanoscale* **2015**, *7*, 18918; c) W. Li, W. Bing, S. Huang, J. Ren, X. Qu, *Adv. Funct. Mater.* **2015**, *25*, 3775; d) T. Park, J. Y. Kim, H. Cho, H. C. Moon, B. J. Kim, J. H. Park, D. Hong, J. Park, I. S. Choi, *Polymers* **2017**, *9*, 140; e) J. H. Park, S. Choi, H. C. Moon, H. Seo, J. Y. Kim, S.-P. Hong, B. S. Lee, E. Kang, J. Lee, D. H. Ryu, I. S. Choi, *Sci. Rep.* **2017**, *7*, 6980.

- [25] W. Zheng, J. Gao, L. Song, C. Chen, D. Guan, Z. Wang, Z. Li, D. Kong, Z. Yang, *J. Am. Chem. Soc.* **2013**, *135*, 266.
- [26] a) J. O. Zoppe, N. C. Ataman, P. Mocny, J. Wang, J. Moraes, H.-A. Klok, *Chem. Rev.* **2017**, *117*, 1105; b) R. Barbey, L. Lavanant, D. Paripovic, N. Schüwer, C. Sugnaux, S. Tugulu, H.-A. Klok, *Chem. Rev.* **2009**, *109*, 5437.
- [27] a) J. Y. Kim, B. S. Lee, J. Choi, B. J. Kim, J. Y. Choi, S. M. Kang, S. H. Yang, I. S. Choi, *Angew. Chem. Int. Ed.* **2016**, *55*, 15306; b) J. Niu, D. J. Lunn, A. Pusuluri, J. I. Yoo, M. A. O'Malley, S. Mitragotri, H. T. Soh, C. J. Hawker, *Nat. Chem.* **2017**, *9*, 537.
- [28] R.-B. Song, Y. Wu, Z.-Q. Lin, J. Xie, C. H. Tan, J. S. C. Loo, B. Cao, J.-R. Zhang, J.-J. Zhu, B. Zhang, *Angew. Chem. Int. Ed.* **2017**, *56*, 10516.
- [29] J. Yang, J. Li, X. Wang, X. Li, N. Kawazoe, G. Chen, *J. Mater. Chem. B* **2016**, *4*, 7662.
- [30] a) S. Sakai, M. Taya, *ACS Macro Lett.* **2014**, *3*, 972; b) Y. Liu, S. Sakai, S. Kawa, M. Taya, *Anal. Chem.* **2014**, *86*, 11592.
- [31] K. Kato, C. Itoh, T. Yasukouchi, T. Nagamune, *Biotechnol. Prog.* **2004**, *20*, 897.
- [32] a) K. Liang, J. J. Richardson, J. Cui, F. Caruso, C. J. Doonan, P. Falcaro, *Adv. Mater.* **2016**, *28*, 7910; b) C. Doonan, R. Riccò, K. Liang, D. Bradshaw, P. Falcaro, *Acc. Chem. Res.* **2017**, *50*, 1423; c) K. Liang, C. Carbonell, M. J. Styles, R. Ricco, J. Cui, J. J. Richardson, D. Maspoch, F. Caruso, P. Falcaro, *Adv. Mater.* **2015**, *27*, 7293; d) K. Liang, R. Ricco, C. M. Doherty, M. J. Styles, S. Bell, N. Kirby, S. Mudie, D. Haylock, A. J. Hill, C. J. Doonan, P. Falcaro, *Nat. Commun.* **2015**, *6*, 7240; e) K. Liang, J. J. Richardson, C. J. Doonan, X. Mulet, Y. Ju, J. Cui, F. Caruso, P. Falcaro, *Angew. Chem. Int. Ed.* **2017**, *56*, 8510.
- [33] a) S. H. Yang, E. H. Ko, Y. H. Jung, I. S. Choi, *Angew. Chem. Int. Ed.* **2011**, *50*, 6115; b) S. H. Yang, K.-B. Lee, B. Kong, J.-H. Kim, H.-S. Kim, I. S. Choi, *Angew. Chem. Int. Ed.* **2009**, *48*, 9160.

- [34] S. Yao, B. Jin, Z. Liu, C. Shao, R. Zhao, X. Wang, R. Tang, *Adv. Mater.* **2017**, *29*, 1605903.
- [35] a) P. T. McKenney, A. Driks, P. Eichenberger, *Nat. Rev. Microbiol.* **2013**, *11*, 33; b) E. Cornejo, N. Abreu, A. Komeili, *Curr. Opin. Cell. Biol.* **2014**, *26*, 132.
- [36] a) R. Ameloot, F. Vermoortele, W. Vanhove, M. B. J. Roeffaers, B. F. Sels, D. E. De Vos, *Nat. Chem.* **2011**, *3*, 382; b) G.-Y. Jeong, R. Ricco, K. Liang, J. Ludwig, J.-O. Kim, P. Falcaro, D.-P. Kim, *Chem. Mater.* **2015**, *27*, 7903; c) A. J. Brown, N. A. Brunelli, K. Eum, f. Rashidi, J. R. Johnson, W. J. Koros, C. W. Jones, S. Nair, *Science* **2014**, *345*, 72.
- [37] a) J. Liu, Y. Lan, Z. Yu, C. S. Y. Tan, R. M. Parker, C. Abell, O. A. Scherman, *Acc. Chem. Res.* **2017**, *50*, 208; b) Z. Yu, J. Zhang, R. J. Coulston, R. M. Parker, F. Biedermann, X. Liu, O. A. Scherman, C. Abell, *Chem. Sci.* **2015**, *6*, 4929; c) R. M. Parker, J. Zhang, Y. Zheng, R. J. Coulston, C. A. Smith, A. R. Salmon, Z. Yu, O. A. Scherman, C. Abell, *Adv. Funct. Mater.* **2015**, *25*, 4091; d) Y. Zheng, Z. Yu, R. M. Parker, Y. Wu, C. Abell, O. A. Scherman, *Nat. Commun.* **2014**, *5*, 5772; e) J. Zhang, R. J. Coulston, S. T. Jones, J. Geng, O. A. Scherman, C. Abell, *Science* **2012**, *335*, 690.
- [38] a) G. Klaufman, R. Boltyanskiy, S. Nejati, A. R. Thiam, M. Loewenberg, E. R. Dufresne, C. O. Osuji, *Lab Chip* **2014**, *14*, 3494; b) R. Huang, S. Wu, Z. Li, *J. Mater. Chem. A.* **2014**, *2*, 1672; c) Q. Ma, Y. Song, J. W. Kim, H. S. Choi, H. C. Shum, *ACS Macro Lett.* **2016**, *5*, 666; d) M. Kim, S. J. Yeo, C. B. Highley, J. A. Burdick, P. J. Yoo, J. Doh, D. Lee, *ACS Nano* **2015**, *9*, 8269; e) S. D. Hann, T. H. R. Niepa, K. J. Stebe, D. Lee, *ACS Appl. Mater. Interfaces* **2016**, *8*, 25603; f) L. Zhang, L.-H. Cai, P. S. Lienemann, t. Rossow, I. Polenz, Q. Vallmajo-Martin, M. Ehrbar, H. Na, D. J. Mooney, D. A. Weitz, *Angew. Chem. Int. Ed.* **2016**, *55*, 13470; g) G. Duan, M. F. Haase, K. J. Stebe, D. Lee, *Langmuir* **2017**, DOI: 10.1021/acs.langmuir.7b01526; h) J. D. de Baubigny, C. Trégouët, T. Salez, N. Pantoustier, P. Perrin, M. Reyssat, C. Monteux, *Sci. Rep.* **2017**, *7*, 1265.

- [39] W. Li, Y. Zhang, Z. Xu, Q. Meng, Z. Fan, S. Ye, G. Zhang, *Angew. Chem. Int. Ed.* **2016**, *55*, 955.
- [40] E. Micheline, L. Cevenini, M. M. Calabretta, S. Spinozzi, C. Camborata, *Anal. Bioanal. Chem.* **2013**, *405*, 6155.
- [41] a) S. H. Yang, J. Choi, L. Palanikumar, E. S. Choi, J. Lee, J. Kim, I. S. Choi, J. H. Ryu, *Chem. Sci.* **2015**, *6*, 4698; b) J. Yang, J. Li, X. Li, X. Wang, Y. Yang, N. Kawazoe, G. Chen, *Biomaterials* **2017**, *133*, 253.
- [42] M. Matsusaki, K. Kadowaki, Y. Nakahara, M. Akashi, *Angew. Chem. Int. Ed.* **2007**, *46*, 4689.
- [43] a) Z. Fazal, J. Pelowitz, P. E. Johnson, J. C. Harper, C. J. Brinker, E. Jakobsson, *ACS Nano*, **2017**, *11*, 3560; b) J. Lee, S. H. Yang, S.-P. Hong, D. Hong, H. Lee, H.-Y. Lee, Y.-G. Kim, I. S. Choi, *Macromol. Rapid Commun.* **2013**, *34*, 1351.
- [44] N. Jiang, X.-Y. Yang, G.-L. Ying, L. Shen, J. Liu, W. Geng, L.-J. Dai, S.-Y. Liu, J. Cao, G. Tian, T.-L. Sun, S.-P. Li, B.-L. Su, *Chem. Sci.* **2015**, *6*, 486.
- [45] V. Maheshwari, D. E. Fomenko, G. Singh and R. F. Saraf, *Langmuir* **2010**, *26*, 371.
- [46] a) S. A. Konnova, Y. M. Lvov, R. F. Fakhrullin, *Langmuir* **2016**, *32*, 12552; b) H. Lee, D. Hong, H. Cho, J. Y. Kim, J. H. Park, S. H. Lee, H. M. Kim, R. F. Fakhrullin, I. S. Choi, *Sci. Rep.* **2016**, *6*, 38517; c) M. R. Dзамukova, E. A. Naumenko, E. V. Rozhina, A. A. Trifonov, R. F. Fakhrullin, *Nano Res.* **2015**, *8*, 2512; d) B. Mattix, T. R. Olsen, Y. Gu, M. Casco, A. Herbst, D. T. Simionescu, R. P. Visconti, K. G. Kornev, F. Alexis, *Acta Biomater.* **2014**, *10*, 623; e) H. Tseng, L. R. Balaoing, G. Grigoryan, R. M. Raphael, T. C. Killian, G. R. Souza, K. J. Grande-Allen, *Acta Biomater.* **2014**, *10*, 173; f) M. R. Dзамukova, E. A. Naumenko, N. I. Lannik, R. F. Fakhrullin, *Biomater. Sci.* **2013**, *1*, 810; g) L. Safarik, K. Pospiskova, K. Horska, M. Safarikova, *Soft Matter* **2012**, *8*, 5407.
- [47] Z. Zhang, E. Ju, W. Bing, Z. Wang, J. Ren, X. Qu, *Chem. Commun.* **2017**, *53*, 8415.
- [48] M. A. K. Jansen, V. Gaba, B. M. Greenberg, *Trends Plant Sci.* **1998**, *3*, 131.

- [49] a) W. Xiong, Z. Yang, H. Zhai, G. Wang, X. Xu, W. Ma, R. Tang, *Chem. Commun.* **2013**, *49*, 7525; b) P. Duan, T. Huang, W. Xiong, L. Shu, Y. Yang, C. Shao, X. Xu, W. Ma, R. Tang, *Langmuir* **2017**, *33*, 2454; c) N. Jiang, X.-Y. Yang, Z. Deng, L. Wang, Z.-Y. Hu, G. Tian, G.-L. Ying, L. Shen, M.-X. Zhang, B.-L. Su, *Small* **2015**, *11*, 2003; d) W. Xiong, X. Zhao, G. Zhu, C. Shao, Y. Li, W. Ma, X. Xu, R. Tang, *Angew. Chem. Int. Ed.* **2015**, *54*, 11961; e) D. Stojkovic, G. Torzillo, C. Faraloni, M. Valant, *Int. J. Hydrogen Energy* **2015**, *40*, 3201.
- [50] a) L. Wang, Z.-Y. Hu, X.-Y. Yang, B.-B. Zhang, W. Geng, G. V. Tendeloo, B.-L. Su, *Chem. Commun.* **2017**, *53*, 6617; b) N. Jiang, G.-L. Ying, S.-Y. Liu, L. Shen, J. Hu, L.-J. Dai, X.-Y. Yang, G. Tian, B.-L. Su, *Chem. Commun.* **2014**, *50*, 15407.
- [51] Z. Chen, H. Ji, C. Zhao, E. Ju, J. Ren, X. Qu, *Angew. Chem. Int. Ed.* **2015**, *54*, 4904.
- [52] C. Guillerey, N. D. Huntington, M. J. Smyth, *Nat. Immunol.* **2016**, *17*, 1025.
- [53] W. Youn, E. H. Ko, M.-H. Kim, M. Park, D. Hong, G. A. Seisenbaeva, V. G. Kessler, I. S. Choi, *Angew. Chem. Int. Ed.* **2017**, *56*, 10702.
- [54] S. H. Yang, E. H. Ko, I. S. Choi, *Langmuir* **2012**, *28*, 2151.
- [55] S. Mansouri, Y. Merhi, F. M. Winnik, M. Tabrizian, *Biomacromolecules* **2011**, *12*, 585.
- [56] B. Wang, G. Wang, B. Zhao, J. Chen, X. Zhang, R. Tang, *Chem. Sci.* **2014**, *5*, 3463.
- [57] Y. Bouhnik, *Lait* **1993**, *73*, 241.
- [58] a) A. J. Priya, S. P. Vijayalakshmi, A. M. Raichur, *J. Agric. Food Chem.* **2011**, *59*, 11838; b) M. B. Thomas, M. Vaidyanathan, K. Radhakrishnan, A. M. Raichur, *J. Food Eng.* **2014**, *136*, 1; c) A. C. Anselmo, K. J. McHugh, J. Webster, R. Langer, A. Jaklenec, *Adv. Mater.* **2016**, *28*, 9486; d) G. Quintana, M. G. Simões, A. Hugo, P. Alves, P. Ferreira, E. Gerbino, P. N. Simões, A. Gómez-Zavaglia, *J. Funct. Food* **2017**, *35*, 408; e) C. Y. Falco, J. Sotres, A. Rascón, J. Risbo, M. Cárdena, *J. Colloid. Interf. Sci.* **2017**, *487*, 97.

- [59] a) K. Kurita, *Mar. Biotechnol.* **2006**, *89*, 2203; b) J. C. Fernandes, F. K. Tavoria, J. C. Soares, O. S. Ramos, M. J. Monteiro, M. E. Pintado, F. X. Malcata, *Food Microbiol.* **2008**, *25*, 922.
- [60] L. Gasperini, J. F. Mano, R. L. Reis, *J. R. Soc. Interface* **2014**, *11*, 20140817.
- [61] M. T. Speth, U. Repnik, G. Griffiths, *Biomaterials* **2016**, *111*, 1.
- [62] a) H. Wang, Z. Feng, B. Xu, *Chem. Soc. Rev.* **2017**, *46*, 2421; b) R. Zhao, B. Wang, X. Yang, Y. Xiao, X. Wang, C. Shao, R. Tang, *Angew. Chem. Int. Ed.* **2016**, *55*, 5225.
- [63] Y. Amano, A. Nishiguchi, M. Matsusaki, H. Iseoka, S. Miyagawa, Y. Sawa, M. Seo, T. Yanaguchi, M. Akashi, *Acta Biomater.* **2016**, *33*, 110.
- [64] W. Li, Z. Liu, C. Liu, Y. Guan, J. Ren, X. Qu, *Angew. Chem. Int. Ed.* **2017**, *56*, 13661.
- [65] a) R. Suntivich, I. Drachuk, R. Calabrese, D. L. Kaplan, V. V. Tsukruk, *Biomacromolecules* **2014**, *15*, 1428; b) I. Drachuk, R. Suntivich, R. Calabrese, S. Harbaugh, N. Kelley-Loughnane, D. L. Kaplan, M. Stone, V. V. Tsukruk, *ACS Biomater. Sci. Eng.* **2015**, *1*, 287.
- [66] a) J. Clausell-Tormos, D. Lieber, J.-C. Baret, A. El-Harrak, O. J. Miller, L. Frenz, J. Blouwolff, K. J. Humphry, S. Kçster, H. Duan, C. Holtze, D. A. Weitz, A. D. Griffiths, C. A. Merten, *Chem. Biol.* **2008**, *15*, 427; b) I. Platzman, J. W. Janiesch, J. P. Spatz, *J. Am. Chem. Soc.* **2013**, *135*, 3339.
- [67] L. Lybaert, K. A. Ryu, R. De Rycke, A. C. Chon, O. De Wever, K. Y. Vermaelen, A. Esser-Kahn, B. G. De Geest, *Adv. Sci.* **2017**, *4*, 1700050.
- [68] E. L. Que, F. E. Duncan, A. R. Bayer, S. J. Philips, E. W. Roth, R. Bleher, S. C. Gleber, S. Vogt, T. K. Woodruff, T. V. O'Halloran, *Integr. Biol.* **2017**, *9*, 135.
- [69] a) C. R. Correia, R. L. Reis, J. F. Mano, *Biomacromolecules* **2013**, *14*, 743; b) R. J. R. W. Peters, M. Marguet, S. Marais, M. W. Fraaije, J. C. M. van Hest, S. Lecommandoux, *Angew. Chem. Int. Ed.* **2014**, *53*, 146; c) M. Marguet, L. Edembe, S. Lecommandoux, *Angew. Chem. Int. Ed.* **2012**, *51*, 1173.

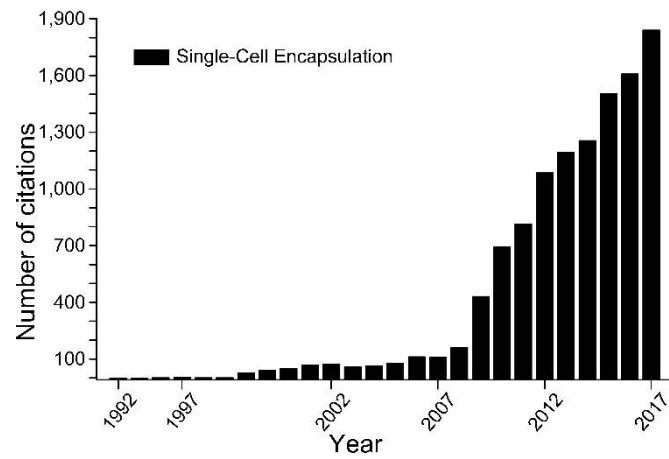


Figure 1. Time evolution of the scientific interest in cell-in-shell structures as illustrated with the number of citations. Each number was obtained by searching ‘single-cell encapsulation’ in Web of Science. For the year 2017, the number has been calculated until 2017 December 16.

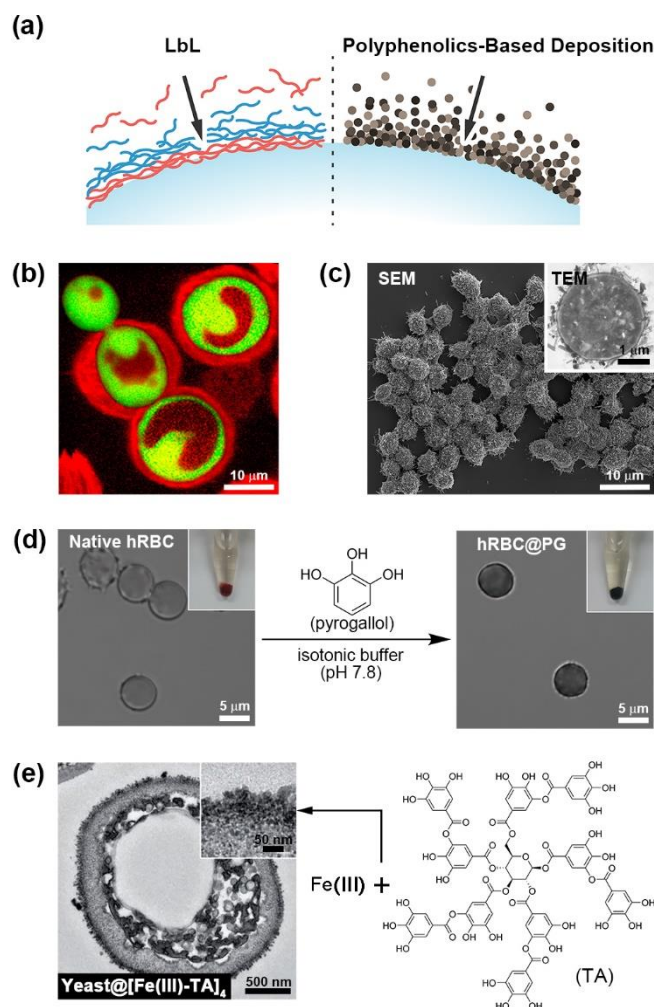


Figure 2. (a) Illustration of “depositing-to” synthetic strategies for cell-in-shell structures with layer-by-layer (LbL) assembly and polyphenolics-based deposition as examples. (b) Confocal laser-scanning microscopy (CLSM) image of yeast cells coated with the cross-linked shell of PVPON/PMAA-*co*-NH₂. PMAA-*co*-Alexa 568 (red) was deposited as a top layer to visualize the shell, and yGFP (green) was expressed with 2% galactose. Reproduced with permission.^[13a] Copyright 2012, American Chemical Society. (c) Scanning electron microscopy (SEM) and transmission electron microscopy (TEM) images of yeast cells coated with halloysite nanotubes. Reproduced with permission.^[14] Copyright 2013, The Royal Society of Chemistry. (d) Optical images of human red blood cells (hRBCs) before and after pyrogallol (PG) coating. Reproduced with permission.^[19] Copyright 2016, Wiley-VCH. (e) TEM image of the microtomed yeast cell that was encapsulated with a complex of Fe(III) and tannic acid (TA). The subscript 4 in the TEM image indicates that the deposition cycle was repeated to four times to obtain the legitimate shell thickness (~40 nm). Reproduced with permission.^[24a] Copyright 2014, Wiley-VCH.

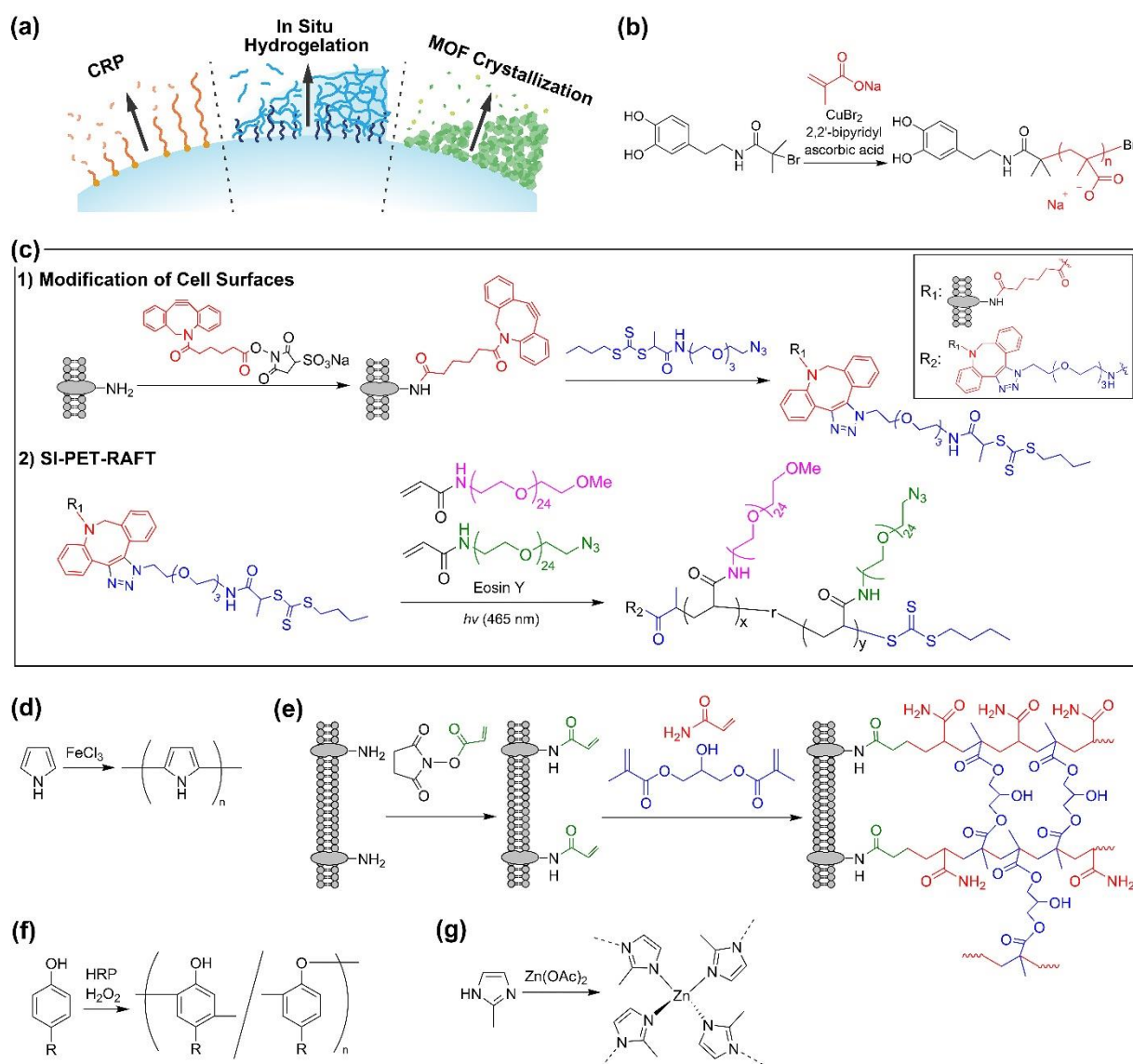


Figure 3. (a) Illustration of “growing-from” synthetic strategies for cell-in-shell structures with surface-initiated, controlled radical polymerization (CRP), in situ hydrogelation, and metal-organic framework (MOF) crystallization as examples. (b-g) Chemical schemes for growing-from strategies. (b) Surface-initiated, activators regenerated by electron transfer ATRP (SI-ARGET ATRP). The dopamine-based ATRP initiator is deposited to cell surfaces and then ARGET ATRP is performed. (c) Surface-initiated, photoinduced electron transfer RAFT (SI-PET-RAFT). The RAFT initiator is covalently linked to the yeast cell-surface, and then PET-RAFT is performed with PEGA-1k (pink) and PEGA-N₃-1k (green) as monomers. (d) In situ polymerization of pyrrole to polypyrrole (PPy) on yeast cells. PPy synthesis is performed after Fe(III) adsorption onto cell surfaces. (e) In situ radical polymerization for formation of cross-linked networks of polymer shells on living cells. Acrylamide (red) and glycerol dimethacrylate (blue) are used in this example. (f) Horseradish peroxidase (HRP)-catalyzed oxidative coupling, in the presence of hydrogen peroxide (H₂O₂), for formation of hydrogel sheath on individual cells. (g) Formation of zeolitic imidazole framework-8 (ZIF-8) for cytoprotective shell formation.

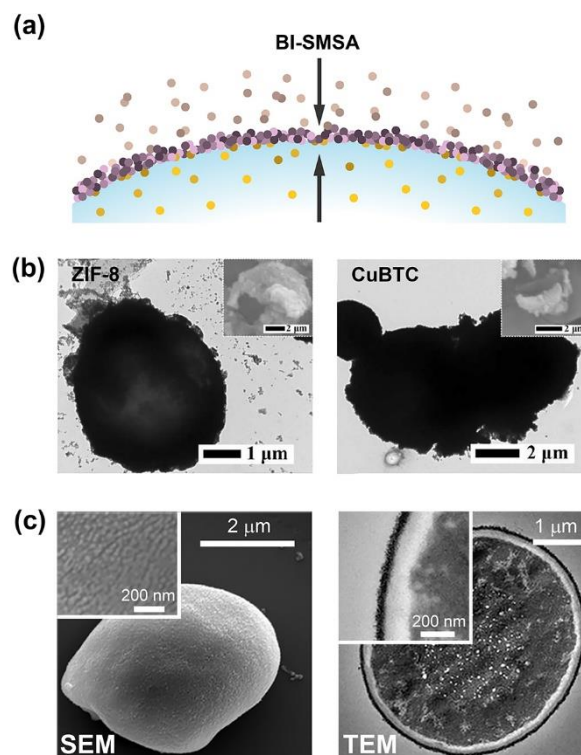


Figure 4. (a) Illustration of biphasic interfacial supramolecular self-assembly (BI-SMSA) for cell-surface engineering. Two layer-forming, self-assembling components (purple and yellow) make a contact with each other at the pericellular space and form the cytoprotective shell. (b) TEM images of hollow MOF microcapsules formed with hollow cell-wall structures as a reservoir for metal ions. Reproduced with permission.^[39] Copyright 2016, Wiley-VCH. (c) SEM and TEM images of yeast@[Fe(III)-TA-MOC] structures, formed by BI-SMSA of Fe(III) and TA. Reproduced with permission.^[23a] Copyright 2017, Wiley-VCH.

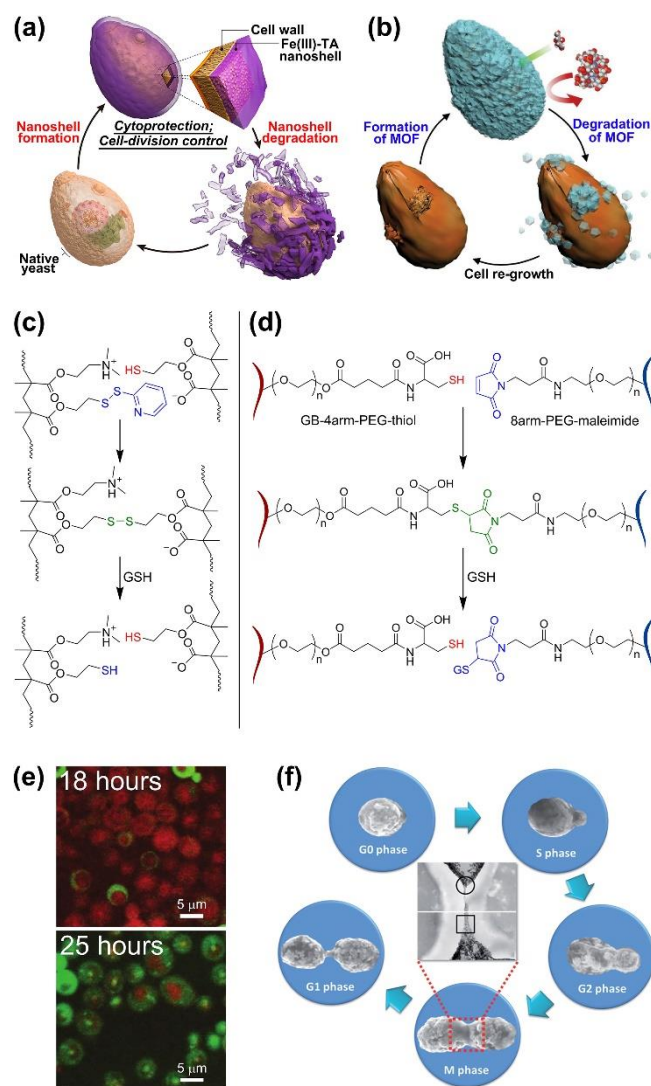


Figure 5. (a and b) Schematic representation of chemical sporulation and germination: (a) yeast@[Fe(III)-TA-MOC] (Reproduced with permission.^[24a] Copyright 2014, Wiley-VCH.) and (b) yeast@[ZIF-8] (Reproduced with permission.^[32a] Copyright 2016, Wiley-VCH.). (c and d) Chemical schemes for formation and degradation of polymeric nanoshells on living cells. In both cases, glutathione (GSH) is used as a degradation inducer: (c) thiol-exchange reaction and (d) combination of thiol-maleimide coupling and retro-Michael-type addition. (e) CLSM images of yeast-in-silk fibroin (SF) structures after 18 h and 25 h of incubation. The fluorescently labeled SF shells (red) are gradually internalized into the yEGFP-expressed yeast cells (green). yEGFP: yeast-enhanced green fluorescent protein. Reproduced with permission.^[12a] Copyright 2013, Wiley-VCH. (f) Self-repairing property of nanoshells composed of AuNP-L-cysteine aggregates during cell cycling. Published by The Royal Society of Chemistry.^[44]

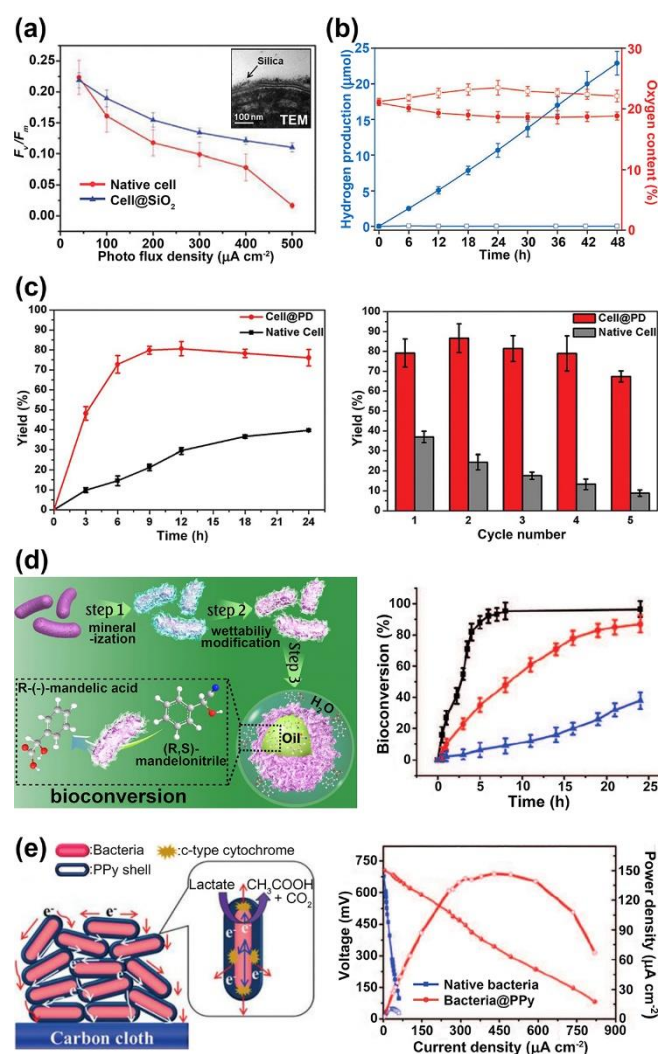


Figure 6. (a) Graphs of maximum quantum yields of PSII (F_v/F_m) vs. photo flux density for native cyanobacteria (*Synechocystis* sp. Strain PCC 6803) and cell@SiO₂. Inset: TEM image of the microtomed cell@SiO₂. Reproduced with permission.^[49a] Copyright 2013, The Royal Society of Chemistry. (b) Graphs of photobiological production of H₂ (blue) and O₂ content (red). Open square: native *Chlorella*; filled circle: *Chlorella*@SiO₂. Reproduced with permission.^[49d] Copyright 2015, Wiley-VCH. (c) (left) (*S*)-1-phenylethanol production yields for the native cell and cell@PD as a function of time and (right) recyclability of the native cell and cell@PD in the production of (*S*)-1-phenylethanol. Reproduced with permission.^[50a] Copyright 2017, The Royal Society of Chemistry. (d) (left) Synthetic scheme of bioconversion of (*R,S*)-mandelonitrile to *R*-(-)-mandelic acid by the robust Pickering interfacial biocatalyst of calcium phosphate (CaP)-encapsulated cells; (right) bioconversion percent under various conditions. Black: Pickering interfacial biocatalysts; red: bacteria in SiO₂-particle-stabilized Pickering emulsions; blue: bacteria in ALG beads. Reproduced with permission.^[51] Copyright 2015, Wiley-VCH. (e) (left) Direct contact-based extracellular electron transfer (EET) mechanism of the bacteria@PPy-deposited carbon cloth anode and (right) polarization and power-density curves of microbial fuel cells (MFCs). Reproduced with permission.^[28] Copyright 2017, Wiley-VCH.

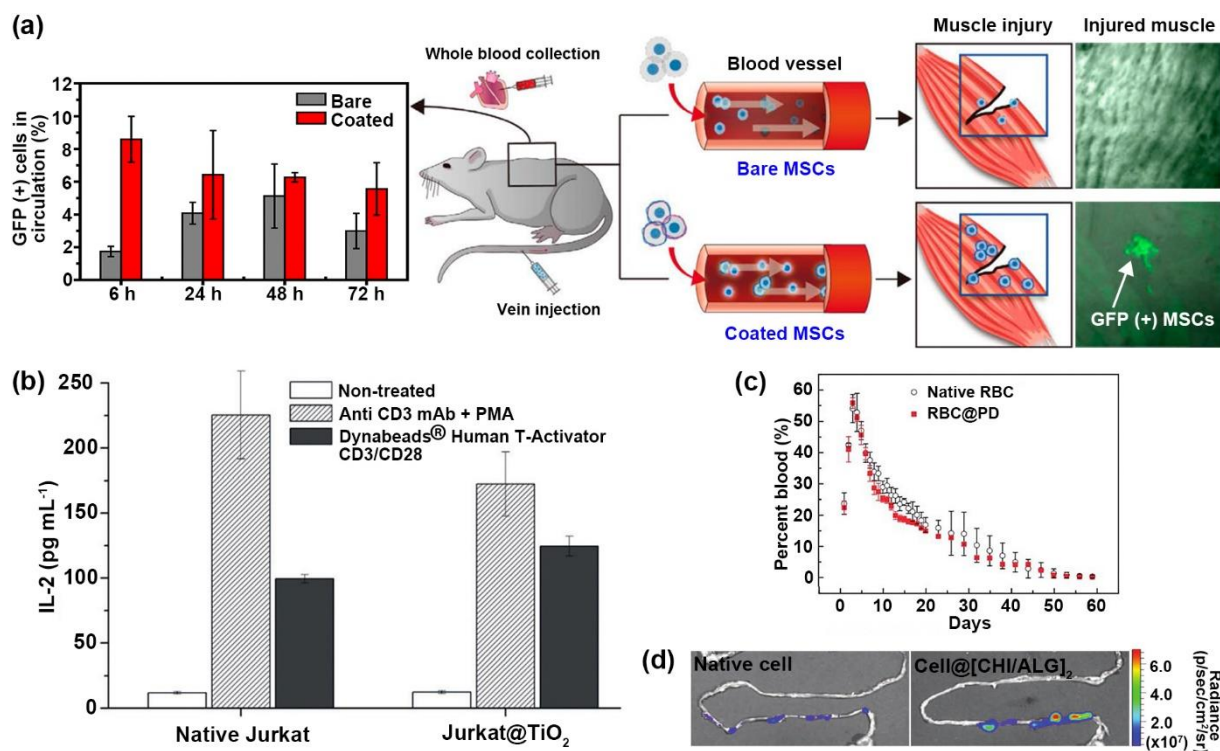


Figure 7. (a) Enhanced in vivo survival and recruitment of nanofilm-coated MSCs, after vein injection, in the muscle-injury mice model. The percentage of GFP (+) MSCs in the blood circulation was analyzed by fluorescence-activated cell sorting (FACS) analysis, and two-photon microscopy images were taken to detect GFP (+) MSCs in slices of the injured muscles. Reproduced with permission.^[15] Copyright 2017, American Chemical Society. (b) Graphs of interleukin-2 (IL-2) secretion from native and Jurkat@TiO₂ after stimulation. PMA: phorbol 12-myristate 13-acetate. Reproduced with permission.^[53] Copyright 2017, Wiley-VCH. (c) In vivo survival profiles of RBCs with three transfusions, indicating the normality of RBC@PD. Published by The Royal Society of Chemistry.^[56] (d) Representative in vivo imaging system (IVIS) spectrums of *Bacillus coagulans* at 1 h after oral gavage, indicating the enhanced in vivo survival of *Bacillus*@[CHI/ALG]₂. Reproduced with permission.^[58c] Copyright 2016, Wiley-VCH.

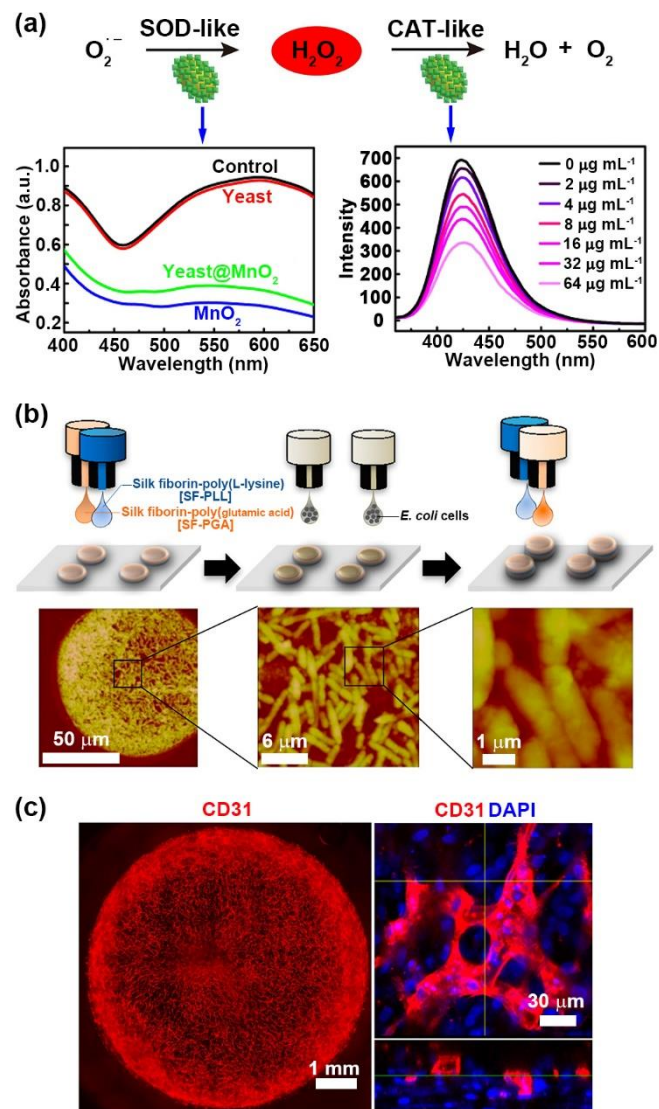


Figure 8. (a) Exogenous catalytic capabilities of yeast@MnO₂: superoxide dismutase (SOD)- and catalase (CAT)-mimetic activities. Reproduced with permission.^[64] Copyright 2017, Wiley-VCH. (b) Atomic force microscopy (AFM) images of (SF-PLL/SF-PGA)₁-*E. coli*-(SF-PLL/SF-PGA)₁ sandwich structures. Reproduced with permission.^[65b] Copyright 2015, American Chemical Society. (c) CLSM images of blood capillary-like networks in 3D-iPSC-CM tissues composed of iPSC-CM, NHCFs, and NHCMECs. NHCMECs were immunostained with anti-CD31 antibody (red), and the nuclei were stained with 4',6-diamidino-2-phenylindole dihydrochloride (DAPI, blue). (right) Top and x,z-reconstructed cross-section images. iPSC: induced pluripotent stem cell; CM: cardiomyocyte; NHCF: normal human cardiac fibroblast; NHCMEC: normal human cardiac microvascular endothelial cell. Reproduced with permission.^[63] Copyright 2016, Elsevier B.V.

Table 1. Demonstrated applications of cell-in-shell structures.

Category	Purpose	Cell type	Shell type	Ref.
Biocatalysis	Photosynthesis	<i>Synechocystis</i> sp. PCC 6803	SiO ₂	49a
	Photosynthesis	<i>C. pyrenoidosa</i>	CeO ₂	49b
	Photosynthesis	<i>Synechococcus</i> PCC 7942	AuNP-L-cysteine/TiO ₂	49c
	Photosynthesis	<i>C. pyrenoidosa</i>	SiO ₂	49d
	Photosynthesis	<i>C. reinhardtii</i>	TiO ₂	49e
	Organic transformation	<i>R. glutinis</i>	PD/M _x O _y	50a
	Organic transformation	<i>Gordonia</i> sp. WQ-01A	AuNP-L-cysteine/TiO ₂	50b
	Organic transformation	<i>A. faecalis</i> ATCC 8750	CaP	51
	Microbial fuel cell	<i>S. oneidensis</i> MR-1	PPy	28
Probiotics	Probiotic delivery	<i>L. acidophilus</i>	CHI/carboxymethyl cellulose	58a
	Probiotic delivery	<i>L. acidophilus</i>	CHI/sulfated β-glucan	58e
	Probiotic delivery	<i>S. boulardii</i>	CHI/dextran sulfate	58b
	Probiotic delivery	<i>B. coagulans</i>	CHI/ALG	58c
	Probiotic delivery	<i>L. delbrueckii subsp. Bulgaricus</i>	CHI/pluronic-PAA	58d
Cell therapy	Stem-cell therapy	MSC	(PLL/HA)/(PLL/RGD)	15
	Immunotherapy	Jurkat	TiO ₂	53
	Immunotherapy	BCG	CHI/poly(l:C)	61
	Immunotherapy	HEK293 / HeLa	CaP	62b
	Blood transfusion	RBC	PD	56
	Blood transfusion	RBC	PG	19
	Blood transfusion	RBC	TA	24d

Author Biographies



Beom Jin Kim is a Ph.D. candidate at the Department of Chemistry, KAIST. He joined the Prof. Choi's group as a graduate student, after obtaining his B.S. degree from the Department of Chemistry, SKKU. His current research interests are biomimetic chemistry, including cell–material interfaces, and interfacial supramolecular self-assembly.



João F. Mano is a Professor at the Department of Chemistry of the University of Aveiro. His current research interests include the use of biomaterials and cells towards the development of transdisciplinary concepts especially aimed at being used in regenerative/personalized medicine or the engineering of microenvironments to control cell behavior and organization. In particular, biomimetic and nano/micro-technology approaches have been applied to nature-derived biomaterials and surfaces in order to obtain biomedical devices with improved structural and functional (including bio-instructive) properties to be used in therapies or in drug screening.



Insung S. Choi is a Professor of Chemistry and of Bio and Brain Engineering at KAIST, and Director of the Center for Cell-Encapsulation Research (Creative Research Initiative). After completing his B.S. and M.S. degrees (with Prof. Eun Lee) at Seoul National University, and his Ph.D. degree (with Prof. George M. Whitesides) at Harvard University, he worked as a postdoctoral researcher (with Prof. Robert Langer) at MIT. His current research interests include biomimetic science and neurochemistry.

Single-cell nanoencapsulation offers a chemical tool for enhancing cell viability in vitro against harmful stresses, promising potential in many applications including biocatalysis and cell therapy. Recent advances in synthetic strategies for forming cell-in-shell structures with unprecedented shell properties are discussed along with demonstrated applications.

Keywords: artificial spores, cell-in-shell, cell nanoencapsulation, cell-surface engineering, interfacial self-assembly

B. J. Kim, H. Cho, J. H. Park, J. F. Mano, I. S. Choi*

Strategic Advances in Formation of Cell-in-Shell Structures: from Syntheses to Applications

